

IAC-12,A6,3,7,x16098

DESIGN AND FABRICATION OF DEBRISAT – A REPRESENTATIVE LEO SATELLITE FOR IMPROVEMENTS TO STANDARD SATELLITE BREAKUP MODELS

**M. Werremeyer**

University of Florida, United States, fg4000@ufl.edu

**Co-Authors**

S. Clark<sup>\*</sup>, N. Fitz-Coy<sup>†</sup>, J.-C. Liou<sup>‡</sup>, M. Sorge<sup>§</sup>, M. Voelker<sup>\*\*</sup>, R. Kelley<sup>††</sup>, T. Huynh<sup>‡‡</sup>

This paper discusses the design and fabrication of Debrisat, a 50 kg satellite developed to be representative of a modern low-Earth orbit satellite in terms of its components, materials used, and fabrication procedures. Debrisat will be the target of a future hypervelocity impact experiment to examine the physical characteristics of debris generated after an on-orbit collision of a modern LEO satellite. The major ground-based satellite impact experiment used by DoD and NASA in their development of satellite breakup models was SOCIT, conducted in 1992. The target used for SOCIT was a Navy transit satellite (40 cm, 35 kg) fabricated in the 1960's. Modern satellites are very different in materials and construction techniques than those built 40 years ago. Therefore, there is a need to conduct a similar experiment using a modern target satellite to improve the fidelity of satellite breakup models. To ensure that Debrisat is truly representative of typical LEO missions, a comprehensive study of historical LEO satellite designs and missions within the past 15 years for satellites ranging from 1 kg to 5000 kg was conducted. This study identified modern trends in hardware, material, and construction practices utilized in recent LEO missions. Although Debrisat is an engineering model, specific attention is placed on the quality, type, and quantity of the materials used in its fabrication to ensure the integrity of the outcome. With the exception of software, all other aspects of the satellite's design, fabrication, and assembly integration and testing will be as rigorous as that of an actual flight vehicle. For example, to simulate survivability of launch loads, Debrisat will be subjected to a vibration test. As well, the satellite will undergo thermal vacuum tests to verify that the components and overall systems meet typical environmental standards. Proper assembly integration techniques will involve precise torqueing of fasteners, thread locking, and the use of appropriate bonding compounds. Finally, the implementation of process documentation and verification procedures is discussed to provide a comprehensive overview of the design and fabrication of this representative LEO satellite.

---

\* University of Florida, United States, [scclark9@ufl.edu](mailto:scclark9@ufl.edu)

† University of Florida, United States, [nfc@ufl.edu](mailto:nfc@ufl.edu)

‡ NASA Orbital Debris Programs Office, United States, [jer-chyi.liou-1@nasa.gov](mailto:jer-chyi.liou-1@nasa.gov)

§ SMC/Aerospace Corporation, United States, [Marlon.E.Sorge@aero.org](mailto:Marlon.E.Sorge@aero.org)

\*\* SMC/Aerospace Corporation, United States, [Michelle.M.Voelker@aero.org](mailto:Michelle.M.Voelker@aero.org)

†† NASA Orbital Debris Programs Office, United States, [robert.l.kelley@nasa.gov](mailto:robert.l.kelley@nasa.gov)

‡‡ SMC/Aerospace Corporation, United States, [Thomas.Huynh@losangeles.af.mil](mailto:Thomas.Huynh@losangeles.af.mil)

## I. INTRODUCTION

The number of man-made objects in Earth orbit has been consistently increasing, and approximately only 6% of the 15,000 traceable objects of larger than 10 cm are active satellites<sup>1</sup>. The remaining objects are debris consisting mainly of retired satellites, upper rocket stages, and remains from on-orbit collisions. The NASA Standard Breakup Model approximates the fragments and orbital debris produced from an on-orbit collision. The accidental collision of the Iridium-33 satellite and retired Cosmos-2251 satellite in 2009 caused a significant increase in the number of debris fragments and reinforced the need to update the NASA Standard Breakup Model. While the current model performed well for the Cosmos-2251 satellite, it underestimated the

number of fragments for the Iridium-33 satellite<sup>2</sup>. The current breakup model was based on a 1992 test and centered on a Navy Transit satellite (~40 cm, 35 kg) fabricated in the 1960's. Modern satellites incorporate many different technologies and materials than satellites designed over 40 years ago. Therefore, there is a need to perform new impact tests with a modern satellite target to improve the fidelity of this model. The design of this satellite, named Debrisat, aims to emulate a representative "next-generation" satellite by incorporating modern technologies such as multi-layer insulation (MLI), composite materials, and coverglass-interconnect cell (CIC) solar panels. The aim of the Debrisat impact test is to provide a better understanding of the Iridium-33 fragments as well as future satellite

breakups. This paper focuses on the design and fabrication of DebrisSat and efforts to ensure that the construction techniques used are consistent with those in modern LEO satellites.

## II. DESIGN

The overall DebrisSat design includes eight major subsystems: structure, attitude determination and control (ADCS), propulsion, electrical power system (EPS), telemetry tracking and command (TT&C), command and data handling (C&DH), thermal management, and payload. The 50 kg design attempts to represent unmanned LEO satellites ranging from 1-5000 kg. Therefore, DebrisSat contains a wide variety of components not typically found on a 50 kg satellite but would be found on satellites in other mass ranges. Thus, the design is not intended to be functional but rather seeks to be representative of component material and functionality as much as possible across a broad range of satellite platforms. The design is shown in Fig. 1.

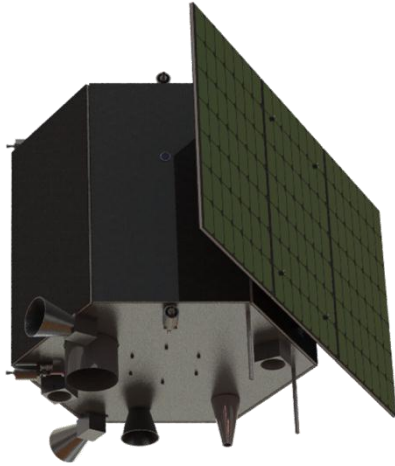


Fig. 1: External view of DebrisSat. The antenna farm on the nadir panel is shown. The solar panels are in the fully deployed position.

The satellite is intended for a hypervelocity impact test at Arnold Air Force Base and is therefore limited by the physical dimensions of the test chamber. As such, a deployable configuration is chosen that does not significantly increase the physical envelope of DebrisSat when deployed. The basic system characteristics of DebrisSat are listed in Table 1.

Project Title:	DebrisSat
Target Mass:	50 kg
Physical Envelope	76 cm (dia.) x 68 cm (ht.)
Stabilization:	3-axis
Deployables:	Yes (partially deployed)

Table 1: Basic characteristics of DebrisSat listed. Since one solar panel will be deployed while the other is stowed, the deployables configuration is considered partially deployed.

As shown in Fig. 2, the satellite is a hexagonal body containing six compartmentalized bays. The nadir and zenith panels are hexagonal, while the side panels are rectangular. Looking down into DebrisSat from the zenith panel, the six side panels are labelled A through F in clockwise fashion, with the deployable solar panel structure mounted to the exterior of panel F. The first six bays are labelled in the same manner, with the seventh bay located in the center of DebrisSat. Bays are separated by vertical ribs.

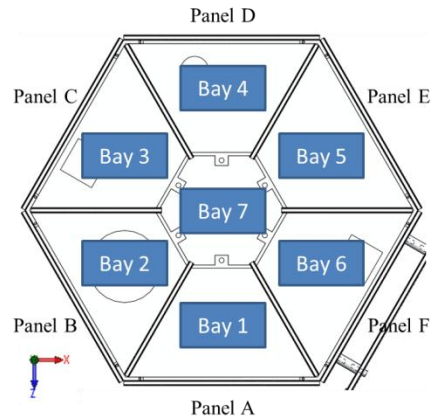


Fig. 2: Internal bay and panel division of DebrisSat. The hexagonal prism design has six side panels, two hexagonal panels, and six ribs that make up the bay and panel divisions.

### II.I Structure

The DebrisSat structure is composed of aluminium and composite structural elements that are intended to give the satellite sufficient strength to withstand launch loads and provide surfaces for mounting the components of other subsystems. Fig. 3 shows the various elements of the DebrisSat structure (excluding solar panels). Two aluminum hexagonal panels form the zenith and nadir panels. Six aluminum longerons at the corner of each hexagon connect the nadir and zenith panels. Six composite side panels complete the hexagonal prism enclosure. Six composite ribs inside the satellite separate the internal bays and provide increased structural rigidity.

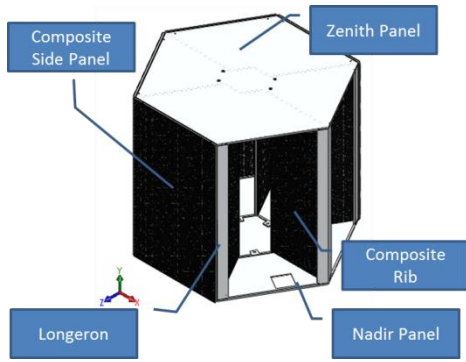


Fig. 3: Two hexagonal panels, six longerons, six composite side panels, and six composite ribs compose the main DebrisSat structure.

The nadir panel design is shown in Fig. 4. The panel has access holes for the optical payload, two spectrometers, and communication antenna. The panel is to be machined out of aluminum 6061-T6 and anodized. The zenith panel is similar in design except it does not have access holes for components since its primary purpose is to serve as a radiator for the thermal management system.

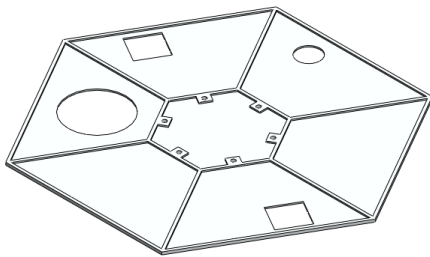


Fig. 4: Aluminum nadir hexagonal panel. The panel includes access and mounting holes for components, as well as webbing for increased structural rigidity.

The longeron is shown in Fig. 5. The design mounts to the hexagonal panels and then composite side panels are mounted to its exterior. The longeron is machined from aluminum 6061-T6 and anodized.

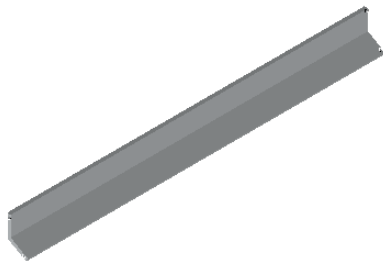


Fig. 5: Aluminum longeron. The longerons connect the hexagonal panels and provide a mounting surface for side panels.

The composite panel design is shown in Fig. 6. The panel consists of carbon fiber face sheets with an aluminum honeycomb core. The carbon fiber face sheets use a quasi-isotropic ply orientation of 0/45/-45/90/90/-45/45/0. Face sheets are to be made from M55J carbon fiber. The honeycomb core is 5 mm thick and made from aluminum 6061-T6 with hexagonal core sizes of 4.76 mm and 0.0254 mm foil thickness. The same composite panel design is used for side panels, solar panels, and ribs, except the footprint of each rib is smaller. Side panels and solar panels are 500 mm by 300 mm while ribs are 490 mm by 200 mm. Two side panels will require heat pipes to be internally laid during their fabrication. Potted inserts will be added to the honeycomb cores to fasten panels to the structure and to connect other subsystem components to the panels.

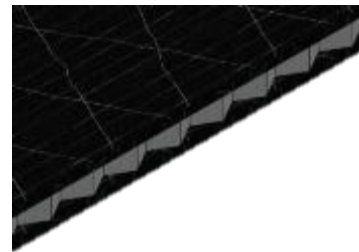


Fig. 6: Composite panel. M55J carbon fiber face sheets with aluminum honeycomb cores are used for the side panels, solar panels, and ribs of DebrisSat.

The deployable solar panel structure is shown in Fig. 7. The center solar panel is connected to panel F using four aluminum standoffs. The two deployable solar panels are connected to the center solar panel using two spring hinges each.

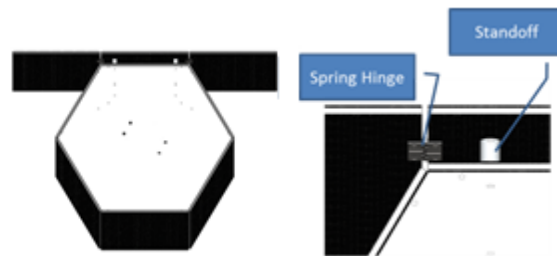


Fig. 7: Deployable solar panel structure. Standoffs are used to connect the center solar panel to DebrisSat, while spring hinges are used to connect the two deployable solar panels.

## II.II Attitude Determination and Control System

For attitude determination, the DebrisSat ADCS utilizes four sun sensors, a three-axis magnetometer, an inertial measurement unit (IMU), and two star trackers. For attitude control, DebrisSat uses four reaction wheels and three magnetorquers.

The sun sensor design is emulated based on the Sinclair digital sun sensor shown in Fig. 8. Four sun sensors are used in the DebrisSat design, three being mounted to composite side panels, and the fourth mounted to the aluminum zenith panel. Each sun sensor mounts with four metric socket cap fasteners and has an anodized aluminum 6061-T6 enclosure. A single D-sub connector connects the sun sensor to an electrical harness. RoHS-compliant BK-7 glass plano-convex lenses are used.

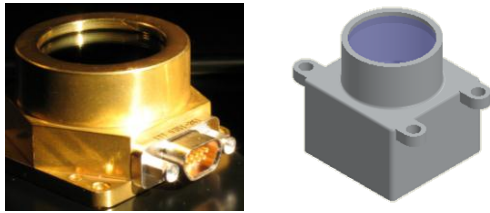


Fig. 8: Sinclair digital sun sensor<sup>3</sup> (left) and emulated sun sensor design (right).

The three-axis magnetometer design is emulated based on the Surrey Satellite Technology magnetometer shown in Fig. 9. The emulated magnetometer uses four metric socket cap fasteners to mount to composite side panel E. The enclosure is made from aluminum 6061-T6 and anodized. A single D-sub connector is used to connect an electrical harness.

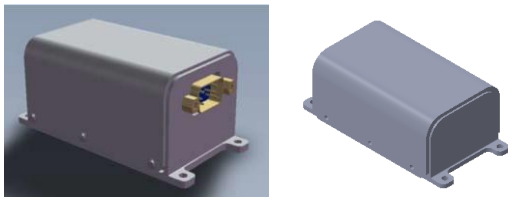


Fig. 9: Surrey magnetometer<sup>4</sup> (left) and emulated magnetometer (right).

A single IMU from Micro Aerospace Solutions is shown in Fig. 10. The same model IMU was donated by Micro Aerospace Solutions and includes an anodized enclosure with two mounting holes (not shown). The IMU is mounted on the aluminum nadir panel using two metric socket cap fasteners and connects to electrical harnesses using an RS485 connection.

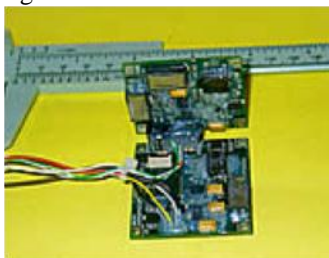


Fig. 10: Micro Aerospace Solutions IMU<sup>5</sup> without enclosure.

The star tracker design is emulated based on the Surrey Satellite Technology star tracker and is shown in Fig. 11. The design uses an anodized aluminum 6061-T6 enclosure and baffle. Four metric socket cap fasteners mount each star tracker to the aluminum nadir panel and a single D-sub connector is connects the star tracker to an electrical harness.



Fig. 11: Surrey star tracker<sup>6</sup> (left) and emulated star tracker (right).

The reaction wheel design is emulated based on the Sinclair Interplanetary 60 mNm-sec reaction wheel and is shown in Fig. 12. One reaction wheel was donated by Sinclair Interplanetary and will be used as a model to emulate the additional three reaction wheels. The emulated design includes a stainless steel flywheel, anodized aluminum 6061-T6 structure, and printed circuit board (PCB). Four metric socket cap fasteners are used to mount the reaction wheels to composite panels and aluminum hexagonal panel. A D-sub connector is used to connect an electrical harness.

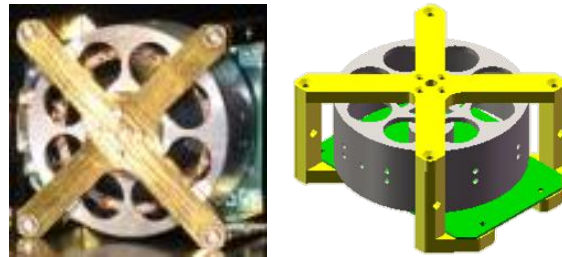


Fig. 12: Sinclair reaction wheel<sup>7</sup> (left) and emulated reaction wheel (right).

The magnetorquer design is based on the Sinclair Interplanetary magnetorquer and is shown in Fig. 13. Sinclair donated three torque rod cores which are used inside of an emulated housing. The housing is made of anodized aluminum 6061-T6 and mounts to the composite ribs using eight metric socket cap fasteners. A D-sub connector is used to connect an electrical harness.



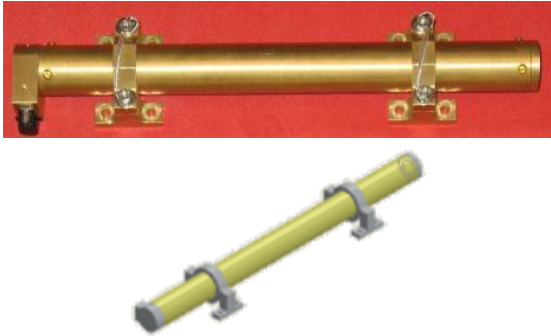


Fig. 13: Sinclair magnetorquer<sup>8</sup> (top) and emulated magnetorquer (bottom).

The emulated ADCS avionics box is shown in Fig. 14. The avionics box uses an anodized aluminum 6061-T6 enclosure and mounts to composite panel E using eight metric socket cap fasteners. The enclosure is 3 mm thick. Internal electronics are emulated using commercial off-the-shelf (COTS) motherboards mounted with wedge locks. Multiple D-sub connectors are used to connect electrical harnesses (not shown).

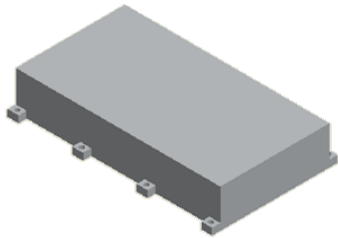


Fig. 14: Emulated ADCS avionics box.

### II.III Propulsion

In order to design a representative propulsion system, the Surrey microsatellite gas propulsion system was examined due to its small size. The Surrey system shown in Fig. 15 utilizes a titanium propellant tank, stainless steel plumbing, solenoids, resistojet thrusters, and cool gas generators. However, the cool gas generators are not expected to be representative for LEO satellites and are therefore not considered in the design. Commercial nitrous oxide kits for automobiles were identified as having similarities with small satellite propulsion systems. The Zex nitrous kit shown in Fig. 15 includes an aluminum tank, nitrous management unit (with electronics and solenoids), injection nozzles, and flexible stainless steel hosing.



Fig. 15: Surrey propulsion system<sup>9</sup> (left) and Zex nitrous kit<sup>10</sup> (right).

Another design consideration was the desire to have a centrally-located propellant tank as a composite overwrapped pressure vessel (COPV) as per the recommendation of a propulsion system subject matter expert (SME)<sup>11</sup>. The resulting emulated COPV design is shown in Fig. 16. The COPV is secured to bay 7 of Debrisat using a primary and secondary mounting bracket. The primary mounting bracket is on the bottom of the COPV and uses a circular bolt pattern to attach to the nadir hexagonal panel. A circular bonding ring is bonded to the outside of the COPV and bolted to the primary mounting bracket. The secondary mounting bracket is mounted near the valve end of the COPV and uses six struts that are bolted to potted-inserts in the vertical composite ribs of the Debrisat structure. The secondary bracket is not bonded to the COPV to allow translation due to relative expansions and contractions between the COPV and the Debrisat structure. Both brackets are anodized aluminum 6061-T6. Metric socket cap fasteners are used for all circular bolt patterns and connections to composite ribs. The composite overwrap is T1000 carbon fiber with a stainless steel pressure vessel underneath.



Fig. 16: COPV with mounting brackets.

The thruster design is emulated based on the resistojet thruster designed by Surrey Satellite Technology and is shown in Fig. 17. The emulated

design has an internal body with nozzle curvature, external heat shell, mounting bracket, and injection nozzle from Zex. All components are stainless steel. Higher temperature alloys such as Inconel® are not used due to the expense of machining. Metric socket cap fasteners are used to secure the thruster to the mounting bracket and the mounting bracket to the DebrisSat structure.



Fig. 17: Surrey resistojet thruster (left)<sup>12</sup> and emulated thruster (right).

The plumbing lines route fuel from the COPV through the solenoids and to the thrusters. Some of the plumbing line routes are shown in Fig. 18. The plumbing navigates around internal components and needs through holes at various locations in the DebrisSat structure. All plumbing lines are stainless steel 316 tubing with 6.35 mm outer diameter and wall thickness of 1.24 mm. All connections are welded and standoffs are located at approximately every 46 cm. The solenoids are housed inside the Zex nitrous management unit, which also serves to emulate the propulsion system avionics.

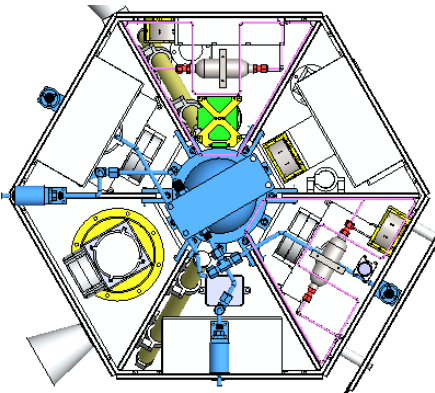


Fig. 18: Propulsion system plumbing routes.

#### II.IV Electrical Power System

The DebrisSat EPS aims to be representative of power generation, storage, and distribution found on LEO satellites. The solar panel design is shown in Fig. 19. Each solar panel has 49 solar cells mounted with NuSil CV-2566 silicon elastomer. The solar cells are 28.3% efficiency CIC ultra-triple-junction (UTJ) obtained as engineering development units (EDUs) from Spectrolab. There are three solar panels on DebrisSat for

a total of 147 solar cells. The solar panel design has carbon fiber face sheets and an aluminum honeycomb core.

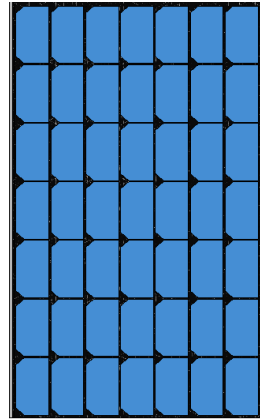


Fig. 19: DebrisSat solar panel.

Power storage is accomplished using three emulated Li-ion battery cases. Although nickel-cadmium and nickel-metal hydride batteries are common in satellite power systems, trends toward increased use of Li-ion cells drove the choice to include Li-ion exclusively. Each battery case is 5 mm thick anodized aluminum and contains ten cylindrical battery cells connected in series. Battery cells are epoxied with thermal compound which helps to transfer heat from the case to the radiator panel. A Pigmat® corrosive absorbent material is included to emulate the mitigation of possible cell discharge. Metric socket cap fasteners hold the case together and mount it to the radiator panel. A single D-sub connector is used to connect a shielded electrical harness. The battery case design is shown in Fig. 20.

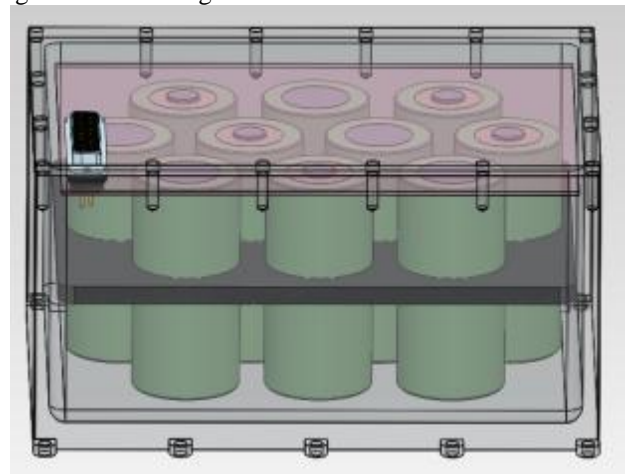


Fig. 20: Emulated Li-ion battery case.

Power conditioning and distribution is handled using an emulated power conditioning and distribution avionics box. Inside, PCBs are used to emulate a battery

charge regulator (one for each battery case), as well as a power condition board and a power distribution board. All power routing is accomplished using D-sub connectors and shielded electrical harness that connect to the solar panels, battery cases, and various components from other subsystems. All electrical harnesses are thermally shielded using Kevlar or braided stainless steel sleeves. The power conditioning and distribution avionics box is shown in Fig. 21

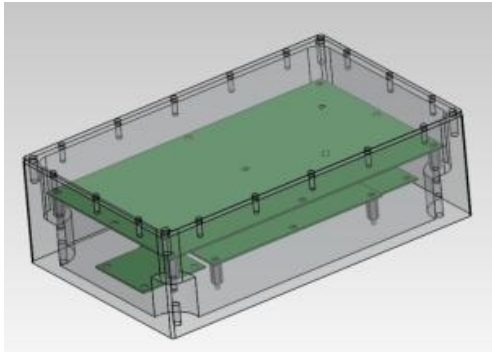


Fig. 21: Power conditioning and distribution avionics box.

#### II.V Telemetry Tracking and Command

The TT&C subsystem includes an emulated S-band antenna, emulated X-band antenna, UHF and VHF antennas, emulated X-band transmitter, and emulated S-band transceiver. The S-band antenna design is based on the Surrey Satellite Technology S-band quadrifilar helix antenna and is shown in Fig. 22. Inside is a coiled copper wire that connects to a standard male RF connector. The base structure is connected to the cone using an adapter ring. The housing is made from anodized aluminum and uses metric socket cap fasteners. A coaxial cable connects the antenna to the S-band transceiver box.

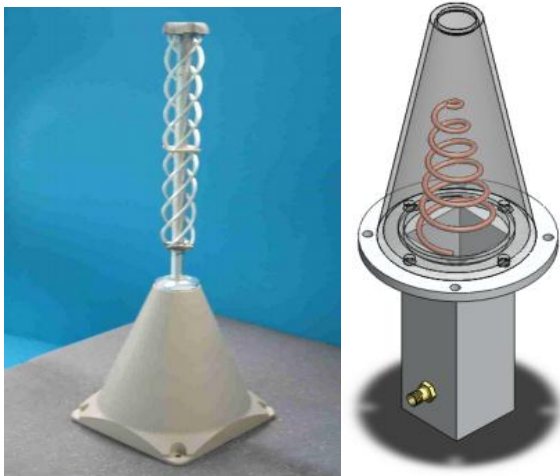


Fig. 22: Surrey S-band quadrifilar helix antenna<sup>13</sup> (left) and emulated S-band antenna (right).

The X-band antenna is emulated based on the Surrey Satellite Technology X-band antenna and is shown in Fig. 23. The emulated antenna has a copper transmission wire that routes to a male RF connector. The base of the antenna is a circular extrusion fastened at a circular mounting ring to an open conical feed horn. The housing is made from aluminum and uses metric socket cap fasteners. A coaxial cable connects the antenna to the X-band transmitter avionics box.

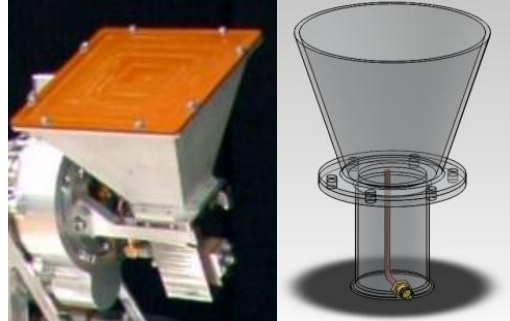


Fig. 23: Surrey X-band antenna<sup>14</sup> (left) and emulated X-band antenna (right).

The UHF and VHF antennas are emulated using a COTS omni-directional whip antenna from DigiKey shown in Fig. 24. The antenna has a copper core wire surrounded by a commercial grade rubber. The appropriateness of the rubber coating will be investigated for use in LEO. Two antennas are used to represent the UHF and VHF frequencies separately.

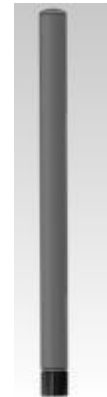


Fig. 24: DigiKey omni-directional whip antenna.

The S-band transceiver and X-band transmitter avionics boxes are emulated using the avionics box design shown in Fig. 25. The avionics box is emulated twice to represent the S-band transceiver and X-band transmitter separately. Inside each box is emulated RF circuitry using two PCBs mounted with standoffs and two COTS signal manipulators. The shielding is

anodized aluminum and uses metric socket cap fasteners. RF connectors receive the coaxial cable from antennas. D-sub connectors are used to connect shielded electrical harnesses.

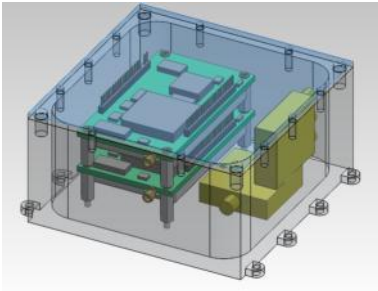


Fig. 25: Emulated S-band transceiver (same as X-band transmitter).

### II.VI Command and Data Handling

The C&DH subsystem is represented by a flight computer avionics box and data recorder avionics box. The flight computer avionics box is shown in Fig. 26. Inside, a single COTS motherboard is used to emulate the flight computer. The shielded enclosure is 3 mm thick anodized aluminum and uses metric socket cap fasteners for mounting and to hold the enclosure together. A D-sub connector is used to connect shielded electrical harnesses.

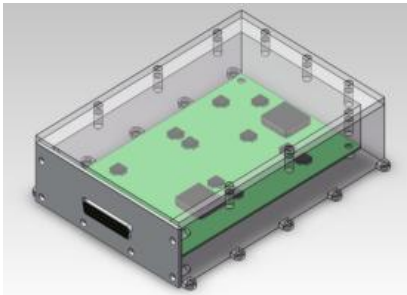


Fig. 26: Emulated flight computer avionics box.

The data recorder is emulated using another COTS motherboard with a shielded enclosure. The data recorder is shown in Fig. 27. The enclosure is 3 mm thick anodized aluminum and uses metric socket cap fasteners for mounting and holding the enclosure together. D-sub connectors are used for connections to shielded electrical harnesses.

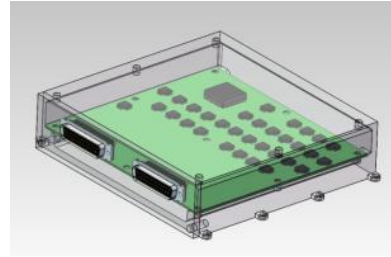


Fig. 27: Emulated data recorder.

### II.VII Thermal Management

The thermal management subsystem emulates capillary pumped loop (CPL) designs for heat pipes, MLI blankets, Kapton heaters, and uses the zenith structural panel as a radiator. Two independent CPLs are used, one in bay 4 and the other in bay 6. The heat pipes must be integrated within the composite panels as shown in Fig. 28.

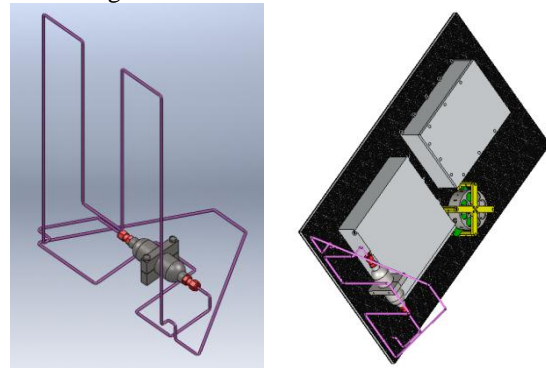


Fig. 28: CPL design (left) and CPL integrated into panel (right).

The CPLs use a custom reservoir and clamp design shown in Fig. 29. The reservoir is made of stainless steel 304 and uses welded connections to connect heat pipes. The clamp is made of stainless steel 316 and uses metric socket cap fasteners to tighten down and to mount to the zenith panel.

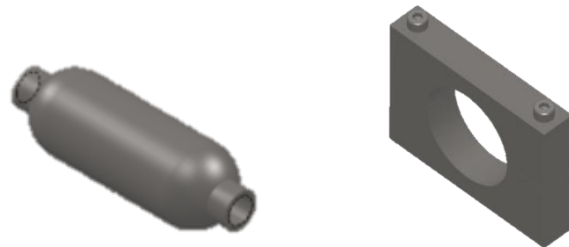


Fig. 29: CPL reservoir (left) and reservoir clamp (right).

MLI is used on the external surfaces of the DebrisSat side panels and nadir panels as shown in blue in Fig. 30, as well as the surface of the emulated optical payload (not shown). The zenith panel does not have MLI coverage since it serves as DebrisSat's radiator. The MLI



will be sewn from 12 layers of metalized polyethylene film interlayered with mesh nylon scrim and placed on each side between two exterior layers of coated polyimide film. The MLI blanket will be made in three to five large pieces with emphasis on minimizing seams and open corners and is attached to the structure using fastening buttons. Approximately 15000 cm<sup>2</sup> of MLI blanket is required to encompass these surfaces.

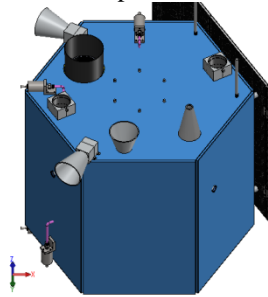


Fig. 30: MLI-covered surfaces shown in blue. MLI also covers side panel F where the solar panels are attached but not the zenith panel.

Kapton heaters are used to maintain the temperature of sensitive avionics. Approximately 2000 cm<sup>2</sup> of internal component surface area will be heated using Kapton heaters. Kapton heaters will be connected to shielded electrical harnesses.

The zenith panel is used as the radiator to reject DebrisSat heat. As discussed in II.I Structure, the panel is made of aluminum 6061-T6, which has desirable conduction and radiation properties. The CPLs use sections of the radiator panel to reject heat from the heat pipes as shown Fig. 31.

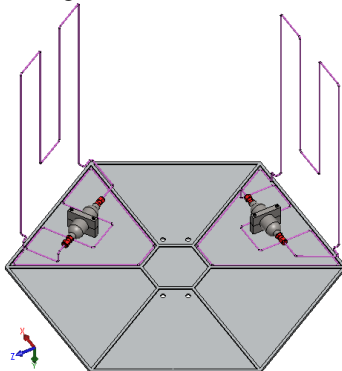


Fig. 31: CPLs integrated into bays on the radiator panel.

## II.VIII Payload

The DebrisSat payload consists of two emulated spectrometers, an emulated optical imager, and a payload support avionics box. The spectrometer design is shown in Fig. 32. It is important to note that the spectrometer design is not intended to be functional, but rather is intended to have the same materials and internal components that would be expected in a LEO

satellite payload. The spectrometer includes a charge-coupled device (CCD) camera, fold-mirror, optical bench, titanium lens mount, and COTS circuitry mounted using wedge locks. Wedge locks were recommended by a payload SME for structurally accepting any payload circuit boards.<sup>15</sup> The spectrometer housing is made of 3 mm thick anodized aluminum and uses metric socket cap fasteners.

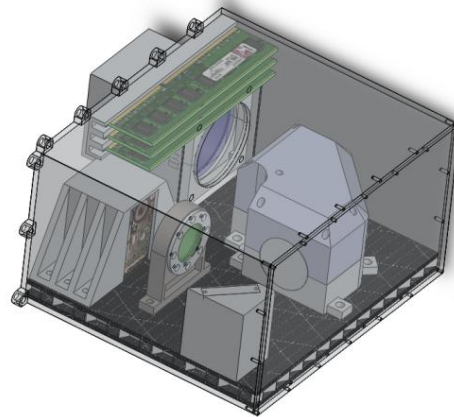


Fig. 32: Emulated spectrometer.

The CCD camera housing is shown in Fig. 33. The CCD camera is emulated using internal components of a digital camera. The housing is webbed and made of anodized aluminum. Socket cap fasteners mount the housing to the optical bench and a D-sub connector is used to connect to electrical harnesses outside of the spectrometer (not shown).

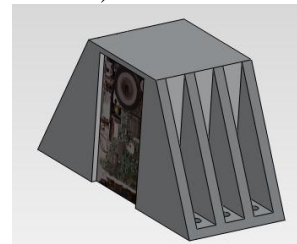


Fig. 33: CCD camera with housing.

The fold mirror is shown in Fig. 34. The fold mirror is emulated using a COTS telescope prismatic fold lens. The fold mirror is enclosed in an anodized aluminum housing and mounted to the optical bench.

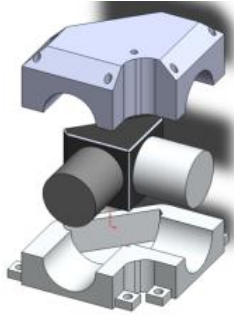


Fig. 34: Fold mirror with housing.

The optical bench is shown in Fig. 35 and was also a recommendation from the payload SME. The optical bench is a composite with M55J carbon fiber face sheets and an aluminum 6063 honeycomb core. The shape of the composite is irregular to encompass the entire floor of the spectrometer housing. Potted-inserts are used in the composite to mount the internal spectrometer components and to mount the optical bench to the spectrometer housing.

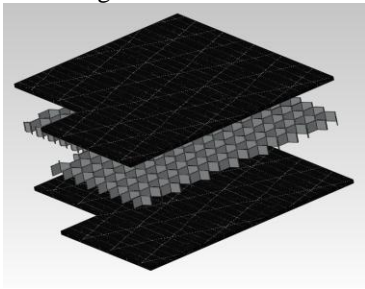


Fig. 35: Optical bench.

The titanium lens mount is shown in Fig. 36. The lens mount is designed with titanium to examine the material's effects on LEO satellite breakups, since some LEO satellites still include limited amounts of titanium in their designs. N-BK7 optical glass is seated in the mount and held in place using an aluminum mounting face.

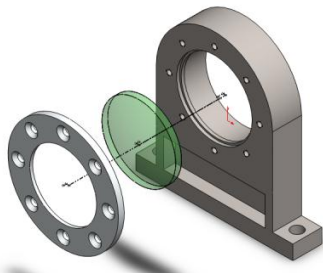


Fig. 36: Titanium lens mount.

The emulated optical imager is shown in Fig. 37. The optical imager includes a modified COTS Cassegrain telescope, CCD camera and electronics, and

sunshade. A custom anodized aluminum adapter encloses the modified Cassegrain telescope and mounts the aluminum sunshade. The sunshade is made of black anodized aluminum.



Fig. 37: Emulated optical imager.

The optics are emulated using a modified COTS Cassegrain telescope from Celestron. The modified COTS telescope is shown in Fig. 38. The external peripherals are removed from the telescope leaving just the aluminum optical tube and internal optics. A custom aluminum three-arm lens brace is manufactured to replace the original brace used to hold the internal reflecting mirror. The three-arm lens brace was recommended by the payload SME.



Fig. 38: Modified Cassegrain telescope.

The CCD camera module is shown in Fig. 39. The CCD camera is emulated using the internal electronics from a digital camera. A custom aluminum lens mount is included that receives light rays from the optical tube. The module is shielded with an anodized aluminum housing and uses a D-sub connector to connect to a shielded electrical harness.

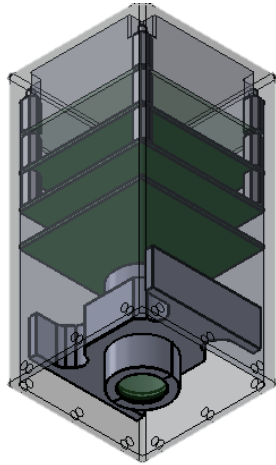


Fig. 39: CCD camera module

Reaction wheels are attached to the outside of the spectrometers and optical imager to emulate jitter control. These reaction wheels are shown for the spectrometer in Fig. 40. The reaction wheels are non-functional but include an anodized aluminum housing, stainless steel flywheel, and axis rod.

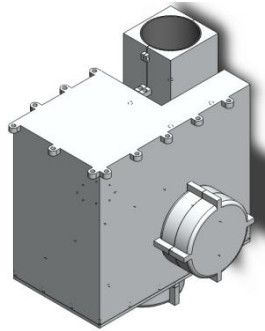


Fig. 40: Reaction wheels attached for jitter control.

The payload support avionics box is shown in Fig. 41. Inside, six COTS motherboards are used to emulate payload avionics. The motherboards are mounted using wedge locks and have six D-sub connectors for connecting to shielded electrical harnesses. Metric socket cap fasteners hold the box together and mount it to the DebrisSat structure. The enclosure is 3 mm thick anodized aluminum.

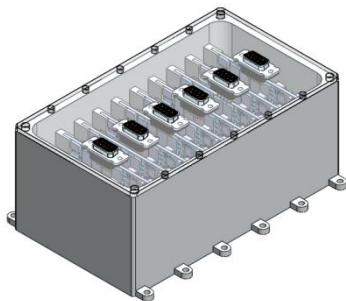


Fig. 41: Payload support avionics box.

### III. ASSEMBLY INTEGRATION AND TESTING

The DebrisSat assembly integration and testing (AI&T) process will follow the DOD-HDBK-343, military standard for “Design, Construction, and Testing Requirements for One of a Kind Space Equipment.” Specifically, all aspects of the assembly integration and testing process will be documented and verified independently during each step of the AI&T process. Testing will be performed according to the latest revision of the NASA General Environmental Verification Standard (GEVS) and will include thermal vacuum and vibration testing. Since DebrisSat is a non-functional design, electrical function and performance and electromagnetic compatibility will not be performed.

The applied manufacturing process controls will include the documentation of all AI&T procedures. Each step of the AI&T procedure will be independently verified upon completion.

All manufactured parts and materials will be subjected to a metrology screen to assure compliance with the specified requirements. The metrology screen will include visual inspection and physical measurements to ensure that all mechanical interfaces are met appropriately and that the parts and materials have do not have excessive nicks, scratches, burrs, corrosion, or contamination. Since components will include special colouring and/or laser etchings for part identification during post-impact characterization, the appropriate color and or laser etchings will also need to be verified at this stage.

Fasteners used in the assembly will be torqued according to the procedure described in the NASA Fastener Design Manual. In addition, thread locking compound will be used in the final torqueing of all fasteners.

Contamination control will be accomplished by performing all assembly procedures at the University of Florida in a 100000 class clean room in the Space Systems Group lab. When not in use, components will be stored in containers in the clean environment.

Thermal vacuum testing will be performed at the University of Florida using a thermal vacuum chamber in the Space Systems Group lab. The thermal vacuum chamber can also be used to sufficiently bake any materials with deleterious outgassing potential. Bonding compounds with low outgassing potential have been selected. Vibration testing will be outsourced and test articles will be subject to additional screening upon completion.

---

<sup>1</sup> M. M. Castronuovo, "Active space debris removal-A preliminary mission analysis and design," *Acta Astronautica*, vol. 69, no. 9-10, pp. 848-859, November-December 2011.

<sup>2</sup> J.-C. Liou, "The Man-Made Orbital Debris Problem and a New Satellite Impact Experiment to Characterize the Orbital Debris Properties," Houston, 2011.

<sup>3</sup> Sinclair Interplanetary, "Digital Sun Sensors," 12 May 2012. [Online]. Available: <http://www.sinclairinterplanetary.com/digitalsunsensors>. [Accessed 13 May 2012].

<sup>4</sup> Surrey Satellite Technology LTD, "Magnetometer," 19 July 2011. [Online]. Available: <http://www.sstl.co.uk/Downloads/Datasheets/Subsys-datasheets/Magnetometer-ST0123582-v1-19->. [Accessed 13 May 2012].

<sup>5</sup> Micro Aerospace Solutions, "Micro Aerospace Solutions," 2012. [Online]. Available: <http://www.micro-a.net/imu.php>. [Accessed 2 August 2012].

<sup>6</sup> Surrey Satellite Technology LTD, "Altair HB+ Star Tracker (Single Unit)," 13 May 2012. [Online]. Available: <http://www.sst-us.com/shop/satellite-subsystems/aocs/altair-hb--star-tracker--single-unit->. [Accessed 13 May 2012].

<sup>7</sup> Sinclair Interplanetary, "Reaction Wheels," 12 May 2012. [Online]. Available: <http://www.sinclairinterplanetary.com/reactionwheels>. [Accessed 13 May 2012].

<sup>8</sup> Sinclair Interplanetary, "Torquers," 12 May 2012. [Online]. Available: <http://www.sinclairinterplanetary.com/torquers>. [Accessed 13 May 2012].

<sup>9</sup> Surrey Satellite Technology, LTD, "Microsatellite Gas Propulsion System," 25 July 2011. [Online]. Available: <http://www.sstl.co.uk/Downloads/Datasheets/Subsys-datasheets/Gas-Propulsion-System-ST0065932-v004-00>. [Accessed 14 February 2012].

<sup>10</sup> Zex, "4-6 Cylinder EFI Wet Nitrous System," 2011. [Online]. Available: <http://www.zex.com/zx/4-6-cylinder-efi-wet-nitrous-system.html>. [Accessed 11 April 2012].

<sup>11</sup> G. Reber, Interviewee, Spacecraft Propulsion. [Interview]. 19 December 2011.

<sup>12</sup> A. Baker, A. da Silva Curiel, J. Schaffner and M. Sweeting, ""You can get there from here": Advanced low cost propulsion concepts for small satellites beyond LEO," 31 May 2005. [Online]. Available: <http://dx.doi.org/10.1016/j.bbr.2011.03.031>. [Accessed 12 August 2012].

<sup>13</sup> Surrey Satellite Technology, "S-band quadrifilar helix antenna," July 2011. [Online]. Available: <http://www.sst-us.com/getdoc/600fbbb1-420b-49a7-9f1a-4dc70100bb2c>. [Accessed 8 August 2012].

<sup>14</sup> Surrey Satellite Technology, "Antenna pointing mechanism (APM) & high gain x-band antenna," July 2011. [Online]. Available: <http://www.sst-us.com/getdoc/57512be8-8ba2-40ba-a1d3-2a180f50c831>. [Accessed 8 August 2012].

<sup>15</sup> P. Thomas, Interviewee, Spacecraft Payloads. [Interview]. 3 May 2012.